

Single versus double bond breakage in a Morse chain under tension: higher index saddles and bond healing

F. A. L. Mauguière*

*School of Mathematics, University of Bristol,
Bristol BS8 1TW, United Kingdom*

P. Collins

*School of Mathematics, University of Bristol,
Bristol BS8 1TW, United Kingdom*

G. S. Ezra

*Department of Chemistry and Chemical Biology, Baker Laboratory,
Cornell University, Ithaca, NY 14853, United States*

S. Wiggins

*School of Mathematics, University of Bristol,
Bristol BS8 1TW, United Kingdom*

(Dated: October 29, 2021)

Abstract

We investigate the fragmentation dynamics of an atomic chain under tensile stress. We have classified the location, stability type (indices) and energy of all equilibria for the general n -particle chain, and have highlighted the importance of saddle points with index > 1 .

We show that for an $n = 2$ -particle chain under tensile stress the index 2 saddle plays a central role in organizing the dynamics. We apply normal form theory to analyze phase space structure and dynamics in a neighborhood of the index 2 saddle. We define a phase dividing surface (DS) that enables us to classify trajectories passing through a neighborhood of the saddle point using the values of the integrals associated with the normal form. We also generalize our definition of the dividing surface and define an *extended dividing surface* (EDS), which is used to sample and classify all trajectories that pass through a phase space neighborhood of the index 2 saddle at total energies less than that of the saddle.

Classical trajectory simulations are used to study single versus double bond breakage for the $n = 2$ chain under tension. Initial conditions for trajectories are obtained by sampling the EDS at constant energy. We sample trajectories at fixed energies both above and below the energy of the saddle. The fate of trajectories (single versus double bond breakage) is explored as a function of the location of the initial condition on the EDS, and a connection made to the work of Chesnavich on collision-induced dissociation. A significant finding is that we can readily identify trajectories that exhibit bond *healing*. Such trajectories pass outside the nominal (index 1) transition state for single bond dissociation, but return to the potential well region, possibly several times, before ultimately dissociating.

PACS numbers: 05.45.-a, 31.15.-p, 34.10.+x, 36.20.-r, 62.25.-g

*Electronic address: Frederic.Mauguiere@bristol.ac.uk

I. INTRODUCTION

There has been much recent interest in the rapidly developing field of ‘mechanochemistry’, where applied force (e.g., tensile stress) is employed to alter absolute rates and/or product ratios of chemical reactions [1–5]. A fundamental understanding of the intramolecular dynamics and reaction kinetics of molecules subject to a tensile force [6–11] is needed to provide a solid theoretical foundation for mechanochemistry, as well as for theories of material failure under stress [12–14], polymer rupture [12, 13, 15–22] adhesion [23], friction [24], and biological applications of dynamical force microscopy [25–31].

Much previous work on the dynamical consequences of the application of tensile stress has focussed on the investigation of fragmentation kinetics of linear chains. Studies of energy transfer and equipartition in single chains of coupled anharmonic oscillators have played an essential role in the development of nonlinear dynamics, beginning with the seminal work of Fermi, Pasta and Ulam [32, 33] (see, for example, refs 34–46).

The dissociation of a 1-D chain subject to constant tensile force is a problem in unimolecular kinetics, and a fundamental issue in unimolecular kinetics concerns the applicability of statistical approaches such as RRKM [47–51] or transition state theory [52–57]. Previous theoretical work has suggested that dissociation of atomic chains under stress is not amenable to simple statistical approaches [40, 58–66]. Early trajectory simulations on the dynamics of Morse chains [58–61] showed that simple bond stretching or force criteria for bond rupture were inadequate, in that apparently broken bonds were observed to reform (*bond healing*). Subsequent simulations of the fragmentation of 1-D Lennard-Jones (LJ) chains at constant strain with inclusion of a frictional damping term and a stochastic force modelling interaction with a heat bath showed that healing of incipient breaks is highly efficient [63] (see also refs 67, 68). Nonexponential decay, failure of RRKM theory, and extensive transition state recrossing effects were found by Bolton, Nordholm and Schranz in their studies of the dissociation of 1-D Morse chains ($N = 2 - 20$) under stress [40].

Standard harmonic classical TST has been applied to the dissociation of a 1-D Morse chain [64, 65], with the transition state for dissociation of a given bond located at the maximum of the effective potential (see below). The *harmonic* canonical TST rate constant did not agree with molecular dynamics calculations, but effects of anharmonicity [40, 51] on the predictions of TST were not systematically investigated. Both RRKM (fully anharmonic, Monte Carlo)

and RRK (harmonic approximation) theory were applied to predict bond dissociation rate constants as a function of energy and tensile force for Morse chains under tensile stress [69]. For chains with $N \geq 3$ atoms a hybrid statistical theory was used involving a harmonic approximation for motion at the transition state for bond dissociation [69]. More recent work has examined isomerization dynamics for a Morse chain under constant strain subject to periodic boundary conditions [70].

Transition state theory, which has long been a cornerstone of the theory of chemical reaction rates [52–57], has been the subject of renewed interest in recent years [71–92]. It has been established both theoretically and computationally that index one saddles [93] of the potential energy surface [94, 95] give rise to a variety of geometrical structures in *phase space*, enabling the realization of Wigner’s vision of a transition state theory constructed in *phase space* [71–92].

Following these studies, attention has naturally focussed on phase space structures associated with saddles of index greater than one, and their possible dynamical significance [96–99]. We have investigated phase space structures and their influence on transport in phase space associated with *index two saddles* of the potential energy surface for n degree-of-freedom (DoF) deterministic, time-independent Hamiltonian systems [96, 99]. We have shown that, for isomerization dynamics in a model $n = 2$ DoF potential, it is possible to distinguish between ‘concerted’ and ‘stepwise’ (or sequential) isomerization trajectories in a dynamically significant way using a normal form Hamiltonian describing the phase space structure in the vicinity of the index 2 saddle. The importance of index 2 saddles for the question of dynamical separability of tight versus roaming mechanisms has recently been established [100]. As discussed in detail in the present paper, higher index saddles arise naturally in the problem of an atomic chain under tensile stress, and we are able to apply the methods and insights from our previous studies to this problem.

In the present work normal form theory together with classical trajectory simulations are used to investigate the fragmentation kinetics and phase space structure of short tethered atomic chains under constant tensile stress. Following previous work, we model the inter-atomic interactions using Morse potentials [69]. Most of our work concerns a ‘chain’ with $n = 2$ particles. Our focus is on the relation between the phase space structure in the vicinity of the index 2 saddle in this system, as described by a normal form Hamiltonian, and the fate of trajectories passing through a suitably defined dividing surface. The competition

between single and double bond breaking is of particular interest, as is the phenomenon of bond ‘healing’ [63, 67, 68].

Our phase space approach to the problem of single versus double bond breakage in the Morse chain under tensile stress is related to the work of Chesnavich on collision induced dissociation [101, 102]; the results obtained in the present paper serve to confirm and extend Chesnavich’s insights concerning the nature of the boundaries between phase space regions associated with single and double bond breakage.

The structure of this paper is as follows. In Sec. II we describe the Hamiltonian for a tethered Morse oscillator chain under tension. We analyze the location and types (indices) of equilibria for the general n -particle chain, and provide numerical results for the $n = 2$ case. Specifically, we note the presence of an index 2 saddle in the 2-atom chain under tensile stress. In Section III we discuss phase space structure and dynamics in a neighborhood of a saddle-saddle equilibrium point. Based on previous work [96, 99], we define a phase space dividing surface (DS) that enables us to classify trajectories passing through a neighborhood of the saddle point using the values of the integrals associated with the normal form. We also generalize our definition of the dividing surface and define an *extended dividing surface* (EDS); the EDS can be used to sample and classify trajectories that pass through a phase space neighborhood of the index 2 saddle at total energies less or greater than that of the saddle. In Section IV we describe our classical trajectory studies of single versus double bond breakage for the $n = 2$ chain under tension. Initial conditions for trajectories are obtained by sampling the EDS at constant energy, and we sample trajectories at fixed energies both above and below the energy of the saddle. The fate of trajectories (single versus double bond breakage) is explored as a function of the location of the initial condition on the EDS. We find that, at the boundary between regions of the EDS associated with trajectories exhibiting breakage of one or the other bond, there is either (i) a region corresponding to double bond breakage, or (ii) a trajectory that is trapped in the vicinity of the potential minimum. The existence of a layer of doubly dissociative trajectories corresponds to the ‘coating’ phenomenon noted by Chesnavich in his work on collision-induced dissociation [101, 102]. Our trajectory results also enable us to identify trajectories that exhibit bond healing; such trajectories pass beyond the nominal (index 1) transition state for single bond dissociation, but return to the well region possibly several times before ultimately dissociating. Section V concludes. The procedure for sampling the DS and EDS used in the computations reported

here is described in detail in Appendix A.

II. MORSE OSCILLATOR CHAIN UNDER TENSION: HAMILTONIAN AND EQUILIBRIA

In this section we describe the Hamiltonian used to model a 1D chain of particles under tensile stress. After deriving the equations of motion, we determine the location of equilibrium points for chains composed of different numbers of particles. We first review the single particle ‘chain’ and then give the general form of the Hamiltonian for the n -particle case together with analysis of equilibria.

A. One particle Morse chain

We consider first a one particle ‘chain’. Although this case is trivial, the results obtained will be useful when dealing with the general case of n -particle chain.

The single degree of freedom (DoF) Hamiltonian for our 1-particle chain is the sum of a kinetic energy term and a potential energy described by a Morse oscillator potential [103] representing a particle of mass m tethered to a wall of infinite mass. To the Morse potential we add a linear term in the bond coordinate representing a tensile force exerted on the particle, whose magnitude is determined by a parameter f . The one DoF Hamiltonian takes the form:

$$H(x, p; f) = \frac{p^2}{2m} + V_M(x) - f(x - x_e) \quad (2.1)$$

where the Morse potential $V_M(x)$ is

$$V_M(x) = D_0[1 - \exp(-\beta(x - x_e))]^2. \quad (2.2)$$

In the following we will measure energies in units of D_0 , the unperturbed Morse dissociation energy, and length in units of x_e , the equilibrium bond distance for zero tensile force. The Morse parameter β will be set equal to $1/x_e$ so that in our units its numerical value is $\beta = 1$.

Associated Hamiltonian equations of motion (vector field) are:

$$\dot{x} = \frac{\partial H}{\partial p} = \frac{p}{m} \quad (2.3a)$$

$$\dot{p} = -\frac{\partial H}{\partial x} = 2D_0\beta\{\exp[-2\beta(x - x_e)] - \exp[-\beta(x - x_e)]\} + f. \quad (2.3b)$$

The equilibrium points of this vector field satisfy the following equations

$$\dot{x}(x, p) = 0 \quad (2.4a)$$

$$\dot{p}(x, p) = 0. \quad (2.4b)$$

Eq. (2.4a) is always satisfied for $p = 0$. The number of (real) roots of eq. (2.4b) depends on the value of the f parameter. The critical value for this parameter is $f_{crit} = D_0\beta/2$, which has the value $f_{crit} = \frac{1}{2}$ in our units. For $0 < f < f_{crit}$ we have two real roots, for $f = f_{crit}$ we have one real root and for $f > f_{crit}$ there is no real root. For $0 < f < f_{crit}$, the two roots are:

$$x_+ = -\frac{1}{\beta} \ln \left(\frac{D_0\beta + \sqrt{D_0^2\beta^2 - 2D_0\beta f}}{2D_0\beta} \right) + x_e \quad (2.5a)$$

$$x_- = -\frac{1}{\beta} \ln \left(\frac{D_0\beta - \sqrt{D_0^2\beta^2 - 2D_0\beta f}}{2D_0\beta} \right) + x_e \quad (2.5b)$$

The equilibrium point $(x_+, 0)$ is the equilibrium phase space point for the Morse oscillator under tensile stress while the $(x_-, 0)$ solution is a saddle point. (The stability of these two solutions can easily be verified by computing the eigenvalues of the matrix associated with the linearization of Hamilton's equations about the equilibrium point of interest.)

For f parameter equal to f_{crit} the two equilibrium points $(x_+, 0)$ and $(x_-, 0)$ merge at a single point, which we will denote by $(x_*, 0)$, in a saddle node bifurcation. For this critical value of f the only real root is

$$x_* = \frac{1}{\beta} \ln(2) + x_e \quad (2.6)$$

As the force parameter $f \rightarrow 0$, $x_+ \rightarrow x_e$, the unperturbed Morse equilibrium distance, while $x_- \rightarrow +\infty$. Figure 1(a) shows the shape of the 1-D potential for values of f parameter between 0 and f_{crit} and Figure 1(b) shows the locations of the different equilibrium points discussed above as a function of f .

B. n -particle Morse chain under tension

We now consider a chain of n particles tethered to an infinite mass wall. For simplicity we assume all particles have the same mass m .

We use two different sets of phase space coordinates to describe the dynamics. The first set of coordinates are 'external' or lab-fixed' variables; the configuration space coordinates

are denoted (x_1, x_2, \dots, x_n) with conjugate momenta $(p_{x_1}, p_{x_2}, \dots, p_{x_n})$. The second set of coordinates are ‘internal’ or bond coordinates; coordinates are denoted $\mathbf{r} = (r_1, r_2, \dots, r_n)$ with conjugate momenta $\mathbf{p}_\mathbf{r} = (p_{r_1}, p_{r_2}, \dots, p_{r_n})$.

Figure 2 shows the definitions of these two coordinate systems for the case of a 2-particle chain. The general relation between coordinates (x_1, x_2, \dots, x_n) and (r_1, r_2, \dots, r_n) is

$$x_k = \sum_{j=1}^k r_j, \quad k = 1, \dots, n. \quad (2.7)$$

The kinetic energy in external coordinates is a diagonal sum of quadratic terms. The potential energy consists of a sum of pairwise Morse interactions between adjacent particles together with potential term linear in the coordinate x_n of the last particle (equivalent to a constant force applied to this particle). The Hamiltonian is therefore

$$H(x_1, \dots, x_n, p_{x_1}, \dots, p_{x_n}; f) = \sum_{i=1}^n \frac{p_{x_i}^2}{2m} + V(x_1, \dots, x_n; f) \quad (2.8)$$

with potential term

$$V(x_1, \dots, x_n; f) = \sum_{i=1}^n V_M(r_i) - f(x_n - nx_e) \quad (2.9a)$$

$$= \sum_{i=1}^n [V_M(r_i) - f(r_i - x_e)] \quad (2.9b)$$

In terms of bond coordinates, the Hamiltonian is (cf. ref. 69)

$$H(\mathbf{r}, \mathbf{p}_\mathbf{r}; f) = \frac{p_{r_1}^2}{2m} + \sum_{i=2}^n \frac{p_{r_i}^2}{m} - \sum_{k=1}^{n-1} \frac{p_{r_k} p_{r_{k+1}}}{m} + V(\mathbf{r}; f). \quad (2.10)$$

The vector field associated with Hamiltonian (2.10) is:

$$\dot{r}_1 = \frac{\partial H}{\partial p_{r_1}} = \frac{p_{r_1}}{m} - \frac{p_{r_2}}{m} \quad (2.11a)$$

$$\dot{r}_i = \frac{\partial H}{\partial p_{r_i}} = \frac{2p_{r_i}}{m} - \frac{p_{r_{i-1}}}{m} - \frac{p_{r_{i+1}}}{m}, \quad i = 2, \dots, n-1 \quad (2.11b)$$

$$\dot{r}_n = \frac{\partial H}{\partial p_{r_n}} = \frac{2p_{r_n}}{m} - \frac{p_{r_{n-1}}}{m} \quad (2.11c)$$

$$\dot{p}_{r_i} = -\frac{\partial H}{\partial r_i} = 2D_0\beta [\exp\{-2\beta(r_i - x_e)\} - \exp\{-\beta(r_i - x_e)\}] + f, \quad i = 1, \dots, n. \quad (2.11d)$$

The equilibrium points are found by setting the time derivatives in eq. (2.11) to zero. The solutions are in fact easily found in terms of equilibrium points for the $n = 1$ DoF system.

$n \backslash k$	0	1	2	3	4	...
0	-					
1	1	1				
2	1	2	1			
3	1	3	3	1		
4	1	4	6	4	1	
\vdots	\vdots	\vdots	\vdots	\vdots	\vdots	\ddots

TABLE I: Pascal's triangle structure of the indices of the different saddles (k) depending on the number of particles in the chain (n). Index 0 means a stable centre (well).

The time derivatives (2.11a), (2.11b) and (2.11c) are zero only for $p_{r_i} = 0$. The solutions obtained by setting the time derivatives of the momenta to zero depend on the value of f parameter. For $0 < f < f_{crit}$ we have two real roots for each r_i which are related with the one DoF roots by $r_{i\pm} = x_{\pm}$, so that the number of equilibria for an n -particle chain is 2^n . The stability of these equilibria is determined by the stability of the one DoF equilibrium points, so that we obtain a c -centre- s -saddle when the x_+ root occurs c times and the x_- root s times with $n = c + s$. The organisation of the different saddle indices follows a Pascal's triangle structure as shown in table I.

In the rest of this paper we focus on the $n = 2$ -particle chain. For this case we have four equilibrium points for $0 < f < f_{crit}$ and only one for $f = f_{crit}$. The situation is summarized as follows:

- $0 < f < f_{crit}$: $EP_1 \equiv (r_{1+}, r_{2+}, 0, 0)$, $EP_2 \equiv (r_{1+}, r_{2-}, 0, 0)$, $EP_3 \equiv (r_{1-}, r_{2+}, 0, 0)$, $EP_4 \equiv (r_{1-}, r_{2-}, 0, 0)$.
- $f = f_{crit}$: $EP_* \equiv (r_{1*}, r_{2*}, 0, 0)$.

EP_1 is a center, $EP_{2,3}$ are index 1 saddles and EP_4 is an index 2 saddle. Figure 3(a) shows contours of the potential function in (r_1, r_2) space as well as the location of the equilibria while Figure 3(b) shows the evolution of the energy of these equilibria points as a function of the force parameter f .

III. PHASE SPACE STRUCTURE AND DYNAMICS IN A NEIGHBORHOOD OF THE INDEX 2 SADDLE

In the present work we focus on the role of the index-2 saddle EP_4 in the bond dissociation kinetics of the 2-particle chain. We study fragmentation dynamics at energies close to the energy of this equilibrium point. Our aim here is to investigate the competition between single and double bond breakage for trajectories that enter the phase space neighborhood of the index 2 saddle. We will study trajectories initiated on a neighbourhood of EP_4 and investigate the dynamical role of the index 2 saddle on the fragmentation of the chain.

In order to carry out this program we construct a normal form Hamiltonian which provides an integrable approximation to the dynamics associated with the original Hamiltonian in a neighbourhood of the saddle point EP_4 . In this section we first briefly describe the construction of a normal form Hamiltonian in a neighbourhood of a saddle point; we then show how this Hamiltonian can be used to describe the dynamics in this neighbourhood and different phase space objects such as normally hyperbolic invariant manifolds (NHIMs), dividing surfaces and extended dividing surfaces (EDS).

A. The normal form

Normal form theory has been mainly applied in reaction dynamics involving equilibrium points of saddle \times center $\times\cdots\times$ center stability type (that is, index 1 saddles). For this kind of saddle the normal form Hamiltonian permits the construction of certain phase space structures which are of central importance for the reaction dynamics (for a review and further references, see ref. 80).

However normal form theory is also useful for describing dynamics in the vicinity of equilibria of different stability type such as EP_4 in the present problem, which is of saddle \times saddle stability type. Recent work has begun to investigate reaction dynamics mediated by higher index saddles [96–99].

The construction of the normal form coordinate set is carried out by Poincaré-Birkhoff normal form theory. The details of this theory are by now well-known and have been presented in detail in a number of reviews and books (see, for example, refs 80, 104). Normal form theory provides an algorithmic procedure for finding a non-linear symplectic change of

variables,

$$(\mathbf{q}, \mathbf{p}) = T(\mathbf{x}, \mathbf{p}_x), \quad (3.1)$$

which will transform a given Hamiltonian into a new, simpler, Hamiltonian,

$$H_{NF}(\mathbf{q}, \mathbf{p}) = H(T^{-1}(\mathbf{q}, \mathbf{p})) = H(\mathbf{x}, \mathbf{p}_x). \quad (3.2)$$

The form of the resulting Hamiltonian H_{NF} is constrained by imposing conditions such as the requirement that H_{NF} should Poisson commute with a certain Hamiltonian H_0 ; in such a case we say that the resulting Hamiltonian is in normal form with respect to this Hamiltonian H_0 . The Hamiltonian H_0 is often taken to have the simplest possible form, namely, a Hamiltonian describing n uncoupled harmonic oscillators.

The normal form Hamiltonian will describe in a neighbourhood \mathcal{L} of the equilibrium point an integrable system which decouples the dynamics into “reaction coordinates” and “bath modes”.

In the general case of a n DoF Hamiltonian system, the matrix associated with the linearization of Hamilton’s equations about the equilibrium point has k pairs of real eigenvalues of equal magnitude, but opposite in sign ($\pm\lambda_i$) and $n - k$ pairs of complex conjugate purely imaginary eigenvalues ($\pm\omega_i$). We will assume that a non-resonance condition holds between the eigenvalues, i.e., the eigenvalues $(\omega_{k+1}, \dots, \omega_n)$ satisfy the relation $c_{k+1}\omega_{k+1} + \dots + c_n\omega_n \neq 0$ for any vector of integers (c_{k+1}, \dots, c_n) . Under these conditions the normalisation procedure transforms the original Hamiltonian to an even order polynomial in the normal form coordinates $(q_1, \dots, q_n, p_1, \dots, p_n)$.

The normal form Hamiltonian thus obtained, H_{NF} , describes an integrable system which approximates the dynamics of the original Hamiltonian H in a neighbourhood of the equilibrium point. As the resulting Hamiltonian is integrable, we can find n integrals of motion and express the normal form Hamiltonian explicitly in terms of these integrals:

$$H_{NF}(\mathbf{q}, \mathbf{p}) = K(I_1, \dots, I_n) \quad (3.3a)$$

$$= \lambda_1 I_1 + \dots + \lambda_k I_k + \omega_{k+1} I_{k+1} + \dots + \omega_n I_n + \text{HOT}, \quad (3.3b)$$

where the higher order terms (HOT) are at least of order two in the integrals (I_1, \dots, I_n) . The expressions of these actions in terms of the normal form coordinates $(q_1, \dots, q_n, p_1, \dots, p_n)$

are:

$$I_i = q_i p_i, \quad i = 1, \dots, k \quad (3.4a)$$

$$I_j = \frac{1}{2}(q_j^2 + p_j^2), \quad j = k + 1, \dots, n. \quad (3.4b)$$

The vector field associated with the normal form Hamiltonian H_{NF} is

$$\dot{q}_i = \frac{\partial H_{NF}}{\partial p_i} = \frac{\partial K}{\partial I_i} \frac{\partial I_i}{\partial p_i} = \Lambda_i q_i \quad (3.5a)$$

$$\dot{p}_i = -\frac{\partial H_{NF}}{\partial q_i} = -\frac{\partial K}{\partial I_i} \frac{\partial I_i}{\partial q_i} = -\Lambda_i p_i, \quad i = 1, \dots, k \quad (3.5b)$$

$$\dot{q}_j = \frac{\partial H_{NF}}{\partial p_j} = \frac{\partial K}{\partial I_j} \frac{\partial I_j}{\partial p_j} = \Omega_j p_j \quad (3.5c)$$

$$\dot{p}_j = -\frac{\partial H_{NF}}{\partial q_j} = -\frac{\partial K}{\partial I_j} \frac{\partial I_j}{\partial q_j} = -\Omega_j q_j, \quad j = k + 1, \dots, n \quad (3.5d)$$

where we have defined the frequencies

$$\Lambda_i = \frac{\partial K}{\partial I_i}, \quad i = 1, \dots, k \quad (3.6a)$$

$$\Omega_j = \frac{\partial K}{\partial I_j}, \quad j = k + 1, \dots, n. \quad (3.6b)$$

We now introduce a new set of canonical coordinates, (Q_i, P_i) , for the saddle planes. These coordinates are useful for describing the dynamics in each saddle plane and are obtained by a canonical transformation of the NF variables (q_i, p_i) $i = 1, \dots, k$

$$Q_i = \frac{1}{\sqrt{2}}(q_i - p_i) \quad (3.7a)$$

$$P_i = \frac{1}{\sqrt{2}}(q_i + p_i), \quad i = 1, \dots, k. \quad (3.7b)$$

In terms of these coordinates the action variables are

$$I_i = \frac{1}{2}(P_i^2 - Q_i^2), \quad i = 1, \dots, k \quad (3.8)$$

while the vector field for the saddle modes transforms to:

$$\dot{Q}_i = \frac{\partial H_{NF}}{\partial P_i} = \frac{\partial K}{\partial I_i} \frac{\partial I_i}{\partial P_i} = \Lambda_i P_i \quad (3.9a)$$

$$\dot{P}_i = -\frac{\partial H_{NF}}{\partial Q_i} = -\frac{\partial K}{\partial I_i} \frac{\partial I_i}{\partial Q_i} = \Lambda_i Q_i, \quad i = 1, \dots, k \quad (3.9b)$$

and the vector field for the bath modes is unchanged.

B. Phase space structures in normal form coordinates

1. Crossing and non-crossing trajectories

The normalization algorithm provides us with an integrable system. The dynamics separates into independent motions in the position-momentum planes for the saddle modes and the bath modes, so that the full dynamics is the cartesian product of the motion in these planes.

There are k saddle ('reactive') planes spanned by coordinates (q_i, p_i) or (Q_i, P_i) , $i = 1, \dots, k$. The phase space for each saddle mode is foliated by manifolds specified by the value of the integral of motion I_i , $i = 1, \dots, k$. For each value of I_i , the trajectory curves (solutions of Hamilton's equations) are simply the two branches of the hyperbola,

$$q_i p_i = \frac{1}{2}(P_i^2 - Q_i^2) = I_i. \quad (3.10)$$

The dynamics in the remaining $n - k$ bath modes consists of uniform rotation in angle θ_j conjugate to the conserved action I_j in the respective (q_j, p_j) planes with $j = k + 1, \dots, n$. The total energy E of the normalized system is a function of the action variables only:

$$K(I_1, \dots, I_n) = E. \quad (3.11)$$

The k saddle integrals I_i , $i = 1, \dots, k$, can either be positive or negative, leading to two different types of branches of the hyperbola in each saddle plane depending on the sign of the integral. For $I_i > 0$ the two branches of the hyperbola form what we call *crossing trajectories* whereas those branches for which $I_i < 0$ are called *non-crossing trajectories*. Considering constant action hyperbolae in the (Q_i, P_i) plane, crossing trajectories are those for which the sign of Q_i changes along the branch whereas non-crossing trajectories are those for which the sign of Q_i remains the same. For crossing trajectories, we can distinguish trajectories for which the sign of Q_i changes from negative to positive from trajectories for which the sign of Q_i changes from positive to negative.

As discussed in ref. 96, we can introduce a symbolic description of trajectories in the neighbourhood of the origin in the saddle plane. A trajectory is labelled by 2 symbols, $(f; i)$, where $i = \pm$, $f = \pm$. Here i refers to the initial sign of Q_j as it enters the neighbourhood of the origin and f refers to the final sign of Q_j as it leaves the neighbourhood. In the case of multiple saddle mode planes, we can extend this symbolic description to $2k$ indices by taking

the cartesian product of the k saddle planes and labelling a trajectory by $(f_1 \dots f_k; i_1 \dots i_k)$. For example, with two saddle modes, a trajectory labelled $(+-; --)$ crosses in the first plane and does not cross in the second plane, the sign of Q_2 remaining negative. Figure 4 shows a schematic representation of the different hyperbola in the two saddle planes.

2. *Dividing surfaces, extended dividing surfaces and NHIMs*

The notion of a dividing surface originates in the study of chemical reaction dynamics. In this context one is interested in defining a surface in phase space separating reactants from products, through which all reactive trajectories must pass, and which is never encountered by any nonreactive trajectories. This surface is conventionally referred to as the transition state (TS). Transition state theory (TST) has a long history going back to Eyring [105], Wigner [52] and Keck [53] (variational transition state theory, introduced in order to deal with the problem of recrossing [55, 56]).

Many chemical applications of TST employ a TS defined in configuration space [57]. For the case of 2 DoF, a dynamically based approach to TST was pioneered by Pechukas, Pollak and Child, who introduced the notion of periodic orbit dividing surface (PODS) [54].

There has been significant recent progress in generalizing the dynamically based PODS approach to obtain a definition of dividing surfaces in phase space for $n \geq 3$ DoF. The phase space approach uses normal form theory to construct a normal form Hamiltonian which reproduces the dynamics in the neighbourhood of the phase space region of interest [80]. This normal form Hamiltonian is the key object which enables the precise mathematical realization of the intuitive idea of a ‘surface of no return’ intersecting all reactive trajectories [71–92].

We now turn to the definition of the dividing surface (DS) and the so-called extended dividing surface (EDS) for the present problem in which there is a dynamically significant index 2 saddle point. The DS and the EDS are codimension one surfaces within the constant energy surface that are transverse to the vector field defined by Hamilton’s equations, and consist of the set of phase space points for which a suitable distance (to be defined) from the equilibrium point is (locally) minimal along the trajectory passing through the phase space point.

Whereas the energy at which the DS is defined cannot be arbitrary, the EDS is defined

for any value of the energy. For simplicity we take the zero of energy to be the energy of the equilibrium point in the neighbourhood of which we compute the normal form Hamiltonian.

We define the square of the distance from the origin *in phase space* to be

$$D \equiv \frac{1}{4} \sum_{i=1}^k (Q_i^2 + P_i^2) \quad (3.12)$$

where the sum is taken over the saddle DoF. (Note that a different definition of the distance D was used in ref. 99. For further discussion of this point, see Appendix A.) Requiring that points on the DS and the EDS are those for which this distance is minimized implies that the time derivative of this distance along the trajectory passing through the phase point should vanish:

$$\dot{D} = \sum_{i=1}^k \Lambda_i Q_i P_i = 0. \quad (3.13)$$

This relation enables us to find those phase space points within a given energy surface that satisfy the (local) minimum distance requirement.

The EDS is defined by the intersection of the following $2n - 1$ dimensional surfaces in the n -dimensional phase space:

$$\begin{aligned} S_1(Q_1, P_1, \dots, Q_k, P_k, q_{k+1}, p_{k+1}, \dots, q_n, p_n) &= K(I_1, \dots, I_n) - E = 0, \\ S_2(Q_1, P_1, \dots, Q_k, P_k, q_{k+1}, p_{k+1}, \dots, q_n, p_n) &= \sum_{i=1}^k \Lambda_i Q_i P_i = 0 \end{aligned} \quad (3.14)$$

The DS is obtained from (3.14) by restricting to points that lie on crossing trajectories. This condition implies that the actions associated with the saddle degrees-of-freedom should be positive. On the other hand, points on the EDS are not required to lie on crossing trajectories so that all phase space points within a given energy surface satisfying the minimum distance requirement belong to the EDS.

In the simplest and most familiar case, a chemical transformation (reaction) involves an equilibrium point of saddle \times centre $\times \dots \times$ centre stability type. The constant energy dividing surface intersects all reactive trajectories and consists of points for which the phase space distance from the saddle point is a minimum. Clearly, for a trajectory to react, the action associated with the saddle mode must be positive in order for the trajectory to overcome

the barrier, whereas the actions relative to the bath are always positive or zero; the energy at which the dividing surface is defined can only be positive. The set of points in a given energy surface which minimize the distance from the saddle equilibrium point are then located precisely on the line $Q_1 = 0$ in the saddle mode plane and in a disk in the bath mode planes. When all the energy is in the saddle direction, the saddle action is a maximum and the actions relative to the bath modes are all zero so that $K(I_{1max}, 0, \dots, 0) = E > 0$. Conversely, when all the energy is distributed amongst the bath modes, the action of the saddle is zero; such phase points do not belong to the DS and in fact constitute a normally hyperbolic invariant manifold, or NHIM [104]. For the case of a 2-DoF system with one saddle mode and one bath mode this NHIM is a periodic orbit, the so-called periodic orbit dividing surface (PODS) [54]. This PODS formally divides the DS into two disjoint pieces: one part for which the reactive trajectories cross the DS from reactants to products (forward reaction) and one piece for which they cross the DS from products to reactants (backward reaction). Again, for a 2-DoF system, each dividing surface (forward/backwards) is a disk, so that the union of the DS and the NHIM is topologically equivalent to a sphere, as represented in Figure 5(a), where the NHIM (PODS) is the equator of this sphere. The NHIM, represented in green, separates the sphere into two hemispheres, the forward (red) and backward (blue) hemispheres.

The phase space definition of the DS is essential for a fundamental understanding of reaction dynamics [54, 80]. On the other hand, if we are interested in characterising all possible types of dynamics in the vicinity of a saddle equilibrium, the DS as defined above does not provide complete information, as (by definition) it intersects only those trajectories which react. In order to define an object which will capture the totality of the dynamics in the phase space neighborhood of the equilibrium point we must extend the notion of a dividing surface by relaxing the restriction to crossing trajectories and so include non-crossing trajectories as well.

This new object is called the *extended dividing surface* (EDS). Formally the definition of this surface is a surface within an energy surface consisting of phase points which (locally) minimize the distance from the saddle point along their trajectory, without any restriction to crossing trajectories. As a consequence, the action associated with the saddle mode can now be either positive or negative. While the DS was only defined for positive energies, the EDS is defined for energies either positive or negative. The topology of the EDS depends,

however, on whether the energy is positive or negative.

Consider the case of an index-1 saddle. For positive values of the saddle action I_1 the EDS is simply the usual DS [99]; that is to say, it is a sphere with forward and backward hemispheres separated by a NHIM. If we allow the saddle action to be negative, for $E > 0$ the equation $K(I_1 < 0, I_2, \dots, I_n) = E > 0$ must be satisfied. In order to compensate for the loss of energy in the saddle direction, the actions of the bath modes have to increase. Topologically the EDS is equivalent to a hyperboloid as represented schematically in Figure 5(b). Notice that in this case the EDS is not compact as the action of the saddle mode can become arbitrarily large and negative, with a corresponding increase of the bath mode actions to conserve energy. Of course this picture is valid only in the neighbourhood of validity of the normal form Hamiltonian and will in general break down outside this neighbourhood. It is important to realise that the EDS only has meaning within this (bounded) neighbourhood of validity for the normal form.

For negative energies the DS is not a subset of the EDS and this EDS is topologically equivalent to a two sheeted hyperboloid represented in Figure 5 (c).

For an index 1 saddle in an n DoF system, the EDS is of subsidiary importance to the DS for understanding phase space structure and reaction dynamics. When we consider the case of higher index saddles, however, the EDS becomes an object of central importance. For this more complex situation the notion of dividing surface itself becomes problematic due to the fact that concepts like ‘reaction pathway’ are not necessarily well-defined (see ref. 100 and refs therein). Even if we retain the strict mathematical definition of the DS as the surface which intersects all reactive trajectories, the resulting surface gives a rather restricted view of the dynamics in the vicinity of the equilibrium point, whereas the EDS is an object encoding all information about the dynamics in the vicinity of the equilibrium.

We now consider in detail the case of an n DoF system with an index 2 saddle. In this case we have two saddle planes and $n - 2$ bath mode planes. For both positive or negative energies we can always find a combination of the different actions which satisfy the equation $K(I_1, I_2, \dots, I_n) = E$ with $I_{1,2}$ positive or negative and the bath actions always positive. Points on the EDS projected onto the saddle plane (Q_i, P_i) can therefore be located on any quadrant of the saddle plane.

Fixing a point in one of the saddle planes, (Q_1, P_1) say, corresponding phase points on the EDS must minimize the distance from the equilibrium point. In Appendix A we describe

our procedure for locating phase points on the EDS at fixed energy. Specifically, we show how a parametrization of the hyperbola describing the NF dynamics in each saddle plane can be used to sample the EDS. Parameters t_i , $i = 1, \dots, k$, describe the position of the phase point on these hyperbolae; a useful representation of the EDS therefore utilizes the space of these t_i parameters.

As discussed in Appendix A, such a representation is multivalued: for every choice of the t_i parameters, there will be several phase space points on the EDS corresponding to different combinations of signs of the actions I_i . It is useful to have a representation of the EDS that retains crucial information such as location of a phase point in the saddle planes and the distance from the equilibrium. In a saddle plane, the character of a trajectory depends on which quadrant the trajectory intersects the EDS. The location of the phase point in the saddle plane can be specified by an angle; for the case of an index 2 saddle there are two angles. We use these two angles and the distance in phase space from the saddle point to construct a toroidal representation of the EDS. Figure 6 shows the definitions of the angles used and the toroidal representation of the EDS. The torus topology is appropriate because phase space points are periodic functions of the angles t_i with period 2π .

As phase points composing the EDS can belong to crossing or non-crossing trajectories, the EDS splits into several parts (four parts for each saddle plane, 4^k parts for an index k saddle). In order to label these different parts of the EDS, we can use the symbolic description defined for crossing and non-crossing trajectories. For the case of $k = 2$ saddle modes the 16 parts of the EDS are labelled by four indices, $(f_1 f_2; i_1 i_2)$. For example, the part of the EDS having trajectories which cross in the first saddle plane and which do not cross in the second saddle plane (with $Q_2 > 0$) is denoted $\text{EDS}_{(++;-+)$. Notice that, according to our definitions, the DS is a subset of the EDS consisting of the parts with symbol codes $(++; --)$, $(+-; -+)$, $(-+; +-)$ and $(--; ++)$.

An important question concerns the method used to sample points on the EDS. One method was described in a previous work [99]. In the present paper we use another sampling method for the EDS, which is described in detail in Appendix A.

IV. SINGLE VERSUS DOUBLE BOND BREAKAGE FOR THE $n = 2$ CHAIN

In this section we use classical trajectories to investigate single versus double bond breakage in the $n = 2$ particle chain. By ‘double bond breakage’, we mean fission of both bonds leading to the complete breakup of the chain. Specifically, we investigate the behavior of trajectories that pass through a neighborhood of the index 2 saddle. Similar dynamics was explored in the pioneering work of Chesnavich on collision induced dissociation reactions [101, 102].

Our problem has two essential parameters. The first is the magnitude f of the tensile force. Varying this parameter changes both the absolute and relative energies of the various equilibrium points: the well (EP_1), the two index one saddles ($EP_{2,3}$), and the index two saddle (EP_4). In the present work we set $f = 0.1$, which represents a physically realistic value of the tensile stress [69]. The other parameter of interest is the energy at which we study the breakage of the chain. Specifically, we are interested in the energy dependence of single versus double breakage of the chain at energies close to the energy of the index two saddle (i.e., near threshold).

To study these questions, we propagate classical trajectories and examine their fate. Points on the EDS (defined as in the previous Section) are used as initial conditions for trajectory propagation. We examine the dependence of the fate of trajectories on their location on the EDS, and attempt to understand the distribution over the EDS in terms of single breakage of either the first or the second bond and double breakage. We also investigate the evolution of this distribution as we change the energy at which the EDS is sampled from an energy greater than that of the index two saddle EP_4 to an energy below. Finally we discuss a possible manifestation and interpretation of the phenomenon of *bond healing* [63, 67, 68] in the light of the behavior found in our classical trajectory simulations.

A. General considerations

To investigate the fate of trajectories at a fixed energy in the neighbourhood of the index 2 saddle EP_4 for the $n = 2$ particle chain, we apply normal form theory to construct a Hamiltonian which approximates the dynamics in a neighbourhood of the equilibrium EP_4 . This equilibrium point is of saddle \times saddle stability type (for $n = 2$ the normal form is a 2

DoF Hamiltonian without bath modes). With this NF Hamiltonian in hand, the sampling of the EDS is carried out using the procedure described in Appendix A. Using the backward transformation from normal form coordinates to physical coordinates defined in equations (3.1) and (3.2), we obtain phase space points belonging to the EDS in the original physical coordinates. We use these points as initial conditions for trajectory propagation, and monitor the fate of each trajectory.

Several different types of trajectory are possible. The first, denoted type 0, are trajectories which remain trapped in the well region in the neighbourhood of equilibrium (minimum) EP_1 over the full integration time. For these trajectories no bonds rupture. The second type of trajectories, denoted type 1, are those which exhibit single bond breakage; those trajectories for which bond r_1 breaks will be denoted type 1_1 and those for which bond r_2 breaks type 1_2 . Finally, type 2 trajectories are those for which both bonds break, corresponding to complete fragmentation of the chain.

One important question concerns the criteria used to decide whether or not a bond has actually broken. In the work reported here, we propagate trajectories for a long time and look at the values of the bond lengths r_1 and r_2 at the end of the run. By choosing thresholds for both r_1 and r_2 coordinates we can determine the trajectory type by comparing the final values of the bond coordinates of the propagated trajectory with suitably chosen values. For our simulations, we integrate trajectories for 2000 time units (time units as defined in Section II) and the thresholds in r_1 and r_2 coordinates were chosen to be 30 (units of r_e).

The matrix associated with the linearisation of Hamilton's equations about the equilibrium point EP_4 has two pairs of real eigenvalues of equal magnitude and opposite signs. For the present problem, with tensile stress parameter $f = 0.1$, these eigenvalues are $\pm\lambda_1 = \pm 0.4972$ and $\pm\lambda_2 = \pm 0.1899$. As is shown in Figure 7, the projections of the associated eigenvectors into the (r_1, r_2) plane indicate reactive directions in the two saddle planes given by the normal form Hamiltonian. Roughly speaking, the 'direction' associated with the first eigenvalue provides in a sense an indicator for which bond will be broken. If we cross the saddle in this eigendirection from negative to positive Q , we will follow the direction given by the eigenvector associated with $+\lambda_1$ and consequently we are likely to break bond r_2 . If we cross in the opposite direction, we follow the direction given by the eigenvector associated with $-\lambda_1$ and are likely to break bond r_1 . The directions corresponding to the eigenvector associated with the second eigenvalue indicate whether the trajectory will enter the well

region (in the neighbourhood of EP_1) or pass into the region where we expect double bond breakage to occur. This crude approach to the dynamics for trajectories entering the vicinity of the index 2 saddle does not capture the full complexity of the dynamics; in fact there is a competition between these two directions in determining the behaviour of the trajectories.

B. Results

1. Energy above the index 2 saddle

We consider first the behaviour of trajectories initiated on the EDS for energies above the energy of the EP_4 saddle point.

To understand our results, we examine the dynamics associated with the second saddle plane in normal form coordinates; roughly speaking, motion along the associated eigendirection determines whether or not the trajectory enters the well region or exits directly into a region of configuration space where we might expect double bond breakage to occur. The normal form Hamiltonian in this plane has 4 distinct types of dynamics (combinations of symbols \pm): two correspond to crossing trajectories and two to non-crossing trajectories. Non-crossing trajectories remain either in the well region ($Q_2 < 0$) or outside the well region ($Q_2 > 0$). There are therefore two relevant classes of trajectories. The first class is composed of trajectories for which the sign of Q_2 changes from negative to positive together with non-crossing trajectories for which $Q_2 > 0$. The second class is composed of trajectories for which the sign of Q_2 changes from positive to negative together with non-crossing trajectories for which $Q_2 < 0$ remain negative. Using the symbolic classification, the first class consists of parts of the EDS associated with codes $(f_1+; i_1-)$ and $(f_1+; i_1+)$, and the second class with codes $(f_1-; i_1+)$ and $(f_1-; i_1-)$, where f_1 and i_1 are used to designate all the possible symbols for the first saddle plane (Q_1, P_1).

Let us focus on the first of these classes, $(f_1+; i_1-) \cup (f_1+; i_1+)$. This class splits into two different subclasses: $(f_1+; i_1-)$ and $(f_1+; i_1+)$. Each of these two subclasses splits in turn into several distinct subclasses according to the symbols associated with motion in the first saddle plane. The first subclass is composed of the parts $(++; +-)$, $(++; --)$, $(-+; --)$ and $(-+; +-)$, whereas the second subclass is composed of the parts $(++; ++)$, $(++; -+)$, $(-+; -+)$ and $(-+; ++)$. The sets of points on the EDS associated with symbol

codes $(++; ++)$ and $(-+; -+)$ are actually empty. This is due to the fact that, when one samples the EDS and tries to solve the equation $K(I_1, I_2) = E > 0$, there is no solution for which the two actions are negative simultaneously.

Figures 8 and 9 show the different parts of the EDS for the two subclasses $(f_{1+}; i_{1-})$ and $(f_{1+}; i_{1+})$. Different types of trajectories on the EDS are represented by different colors: red for type 1_2 , green for type 1_1 and blue for type 2.

The interpretation of these results is quite clear. The fate of trajectories in each of these subclasses is apparently controlled to a large extent by the dynamics associated with the first saddle plane. Classifying the results according to the symbols in this plane, trajectories in the subclass $(++; +-)\cup(++; --)$ exhibit mainly type 1_2 behavior, as expected for trajectories which either cross the first saddle direction from $Q_1 < 0$ to $Q_1 > 0$ or from trajectories which remain on the half of the plane (Q_1, P_1) with $Q_1 > 0$. Referring to Figure 7, we see that these trajectories are those for which the bond r_2 is anticipated to break. In the same manner, trajectories in the subclass $(-+; --)\cup(-+; +-)$ are mainly type 1_1 .

An important observation is the fact that type 2 trajectories (those exhibiting double bond fission) are not distributed randomly on these parts of the EDS; rather, type 2 trajectories actually occur at the *boundary* between type 1_1 and 1_2 (cf. refs 101, 102).

We now turn to the second class of trajectory, consisting of sets $(f_{1-}; i_{1+})\cup(f_{1-}; i_{1-})$. Again, this class splits into two subclasses $(f_{1-}; i_{1+})$ and $(f_{1-}; i_{1-})$, and those subclasses split again according to the dynamics in the first saddle plane. Figures 10 and 11 show the results for these two subclasses. The situation is now very different from the previous case. All the trajectories belonging to these two subclasses enter the well region. The subsequent dynamics is then much more complex, and we are unable to predict which bond will be broken for a trajectory initiated on this portion of the EDS.

It should nevertheless be emphasized that the distribution of the different types of trajectory within these parts of the EDS is by no means random and that we readily recognize a pattern of red and green ‘stripes’, corresponding to alternating single bond breakages. The interesting question then arises as to what happens at the boundary between types 1_1 and 1_2 . In order to answer this question we sampled a line of initial conditions on the EDS which intersects these alternation of red and green strips. The results are shown in figure 12. Figure 12(a) shows trajectory type versus the P_1 coordinate (used to sample the line of initial conditions); the results indicate an alternation of the two types 1_1 and 1_2 . On

the scale of Figure 12(a), the transition between one type to the other seems to be abrupt; however, sampling more densely we get the results shown on Figure 12(b), where now type 2 behaviour appears at the boundary between type 1_1 and 1_2 .

The interpretation of this result is again very simple. As the energy at which we sample the EDS is greater than the energy of the EP_4 saddle, trajectories in principle have enough energy to pass over the index 2 saddle and break 2 bonds. By continuity, as we pass from the set of initial conditions in which the single bond r_1 breaks to the set where bond r_2 breaks, we traverse the region of the EDS where both bonds break (cf. again the work of Chesnavich, refs 101, 102).

2. Energy below the index 2 saddle and ‘bond healing’

We now turn to the behavior of trajectories initiated on the EDS at energies below the energy of the equilibrium EP_4 .

As discussed in the previous subsection, the results are easier to understand if we consider separately the part of the EDS consisting of trajectories which immediately escape from the well region and the part for which trajectories enter the well.

As before, the first class of trajectories is $(f_1+; i_1-)\cup(f_1+; i_1+)$. As for the higher energy case, type 2 trajectories appear at the boundary between types 1_1 and 1_2 and we obtain mainly type 1_1 behavior for subsets having symbols $(-; +)$ and $(-; -)$ for motion in saddle plane 1 and conversely mainly type 1_2 for subsets having symbols $(+; +)$ and $(+; -)$. These two subclasses are represented on figures 13 and 14

The second class, as for the case of energies above that of the saddle, show a complex dynamics with alternation of type 1_1 and 1_2 trajectories. The two subclasses of this class are represented on figure 15 and 16. Again, our interest will focus on what happens at the boundary. If we sample along a line of initial conditions we see an abrupt change between these types; however, even if we sample on a very fine grid we do *not* see type 2 trajectories at the boundary. Figure 17 shows the global representation of the EDS in the toroidal representation at energy $E = -0.03$.

In Figure 18 we examine the trajectory exit time (the time it takes for a trajectory to actually dissociate, either along bond r_1 or r_2) along the line of initial conditions. Figures 18(a), (b) show the trajectory type and corresponding exit time, respectively, along the

sampling line. At the boundary between types 1_1 and 1_2 , the exit time becomes very large, and appears to diverge as the sampling density is increased (results not shown here). We conclude that, at the boundary between type 1_1 and 1_2 trajectories, there exists a set of measure zero for which the exit time is infinite. In other words, these are trajectories that are trapped in the well region for $t \rightarrow +\infty$. The interpretation of this result is quite familiar [54]: trajectories do not have enough energy to overcome the barrier for double bond breakage so that, in order to dissociate, either the r_1 bond or the r_2 bond must break. Between these 2 possibilities, we have trajectories that take an infinite time to ‘decide’ between dissociation channels, and so remain trapped in the well. (Note that, although we initiate trajectories in the vicinity of index 2 saddle, trajectories can dissociate either by passing close to the index 2 saddle or by passing through the ‘usual’ transition state associated with one of the index 1 saddles. In the present work, we do not explore the interesting and important dynamical interplay between index 1 and index 2 saddles (cf. ref. 100), nor do we investigate the possibility of defining a ‘global’ dividing surface encompassing both types of saddle [100].)

Examination of those trajectories which exhibit a large exit time suggests a connection between the form of these trajectories in configuration space and the so-called *bond healing* phenomenon [63, 67, 68].

Figure 19 shows two examples of trajectories having a large exit time. The phenomenon of bond healing (as we interpret previous discussions [63, 67, 68] of the concept) refers to the incipient breakage of one bond of the chain, followed by a recombination or ‘healing’ of the bond rather than dissociation. The trajectories shown in Figure 19 exhibit precisely this behavior; the trajectories pass well outside the nominal transition state (index 1 saddle) before returning to the well region before ultimately dissociating. In fact, these trajectories exhibit what might be called alternating bond healing, where one bond almost breaks and then reforms and then the other bond breaks and reforms, and so on and recombined. Such trajectories oscillate in an anti-diagonal direction in the (r_1, r_2) plane.

An important task for future investigation is the identification and computation of invariant phase space objects (periodic orbits, NHIMs) which are responsible for trapping trajectories in their vicinity, leading to divergent exit times.

V. CONCLUSIONS AND PERSPECTIVES

In this paper we have investigated the fragmentation dynamics of an atomic chain under tensile stress. We have analyzed the location and types (indices) of equilibria for the general n -particle chain, and have noted the importance of saddle points with index > 1 .

For an $n = 2$ -particle chain under tensile stress the index 2 saddle is of key significance for the dynamics. Building upon previous work, we apply normal form theory to analyze phase space structure and dynamics in a neighborhood of the index 2 saddle. We define a phase dividing surface (DS) that enables us to classify trajectories passing through a neighborhood of the saddle point using the values of the integrals associated with the normal form. We also generalize our definition of the dividing surface and define an *extended dividing surface* (EDS), which is used to sample and classify trajectories that pass through a phase space neighborhood of the index 2 saddle at total energies less than that of the saddle.

Classical trajectory simulations are used to study single versus double bond breakage for the $n = 2$ chain under tension. Initial conditions for trajectories are obtained by sampling the EDS at constant energy. We sample trajectories at fixed energies both above and below the energy of the saddle. The fate of trajectories (single versus double bond breakage) is explored as a function of the location of the initial condition on the EDS, and connection made to the work of Chesnavich on collision-induced dissociation [101, 102]. A significant finding is that we can readily identify trajectories that exhibit bond *healing* [63, 67, 68]; such trajectories pass outside the nominal transition state for single bond dissociation, but return to the well region possibly several times before ultimately dissociating. Identification of the invariant phase space structures associated with trapped trajectories is a topic for future investigation.

Acknowledgments

FM, PC, and SW acknowledge the support of the Office of Naval Research (Grant No. N00014-01-1-0769) and the Leverhulme Trust.

Appendix A: Sampling the extended dividing surface for index k saddles

The concept of the extended dividing surface (EDS) (as introduced in Section III) is of essential importance for our study. The precise definition of this phase space object is given in terms of the normal form Hamiltonian. A procedure for sampling phase space points on the dividing surface associated with index-2 saddles was introduced and implemented in Ref. 99. In this Appendix we present another method of sampling the Normal Form EDS which extends quite naturally to the case of index k saddles where $k \geq 2$.

We start by recalling the definition of the saddle actions in terms of the (Q_i, P_i) coordinates:

$$I_i = \frac{1}{2}(P_i^2 - Q_i^2), \quad i = 1, \dots, k. \quad (\text{A1})$$

As the actions I_i are constants of the motion, we have in each saddle plane the equation:

$$\frac{P_i^2}{2I_i} - \frac{Q_i^2}{2I_i} = 1, \quad (\text{A2})$$

which is just the equation of a doubly-branched hyperbola. There is then a very simple parametrization of the hyperbola in terms of one parameter t_i , where the form of the parametrization depends on the sign of I_i . For the case $I_i > 0$ we have:

$$Q_i = \sqrt{2I_i} \tan(t_i) \quad (\text{A3a})$$

$$P_i = \frac{\sqrt{2I_i}}{\cos(t_i)}, \quad t_i \in \left] \frac{-\pi}{2}; \frac{\pi}{2} \right[\cup \left] \frac{\pi}{2}; \frac{3\pi}{2} \right[. \quad (\text{A3b})$$

while for $I_i < 0$ we take:

$$Q_i = \frac{\sqrt{2|I_i|}}{\cos(t_i)} \quad (\text{A4a})$$

$$P_i = \sqrt{2|I_i|} \tan(t_i), \quad t_i \in \left] \frac{-\pi}{2}; \frac{\pi}{2} \right[\cup \left] \frac{\pi}{2}; \frac{3\pi}{2} \right[. \quad (\text{A4b})$$

In ref 99 the dividing surface was defined as a codimension one surface within the energy surface consisting of phase points which minimized the distance from the origin, where the distance \bar{D} was defined in configuration (Q_i) space:

$$\bar{D} = \frac{1}{2} \sum_{i=1}^k Q_i^2. \quad (\text{A5})$$

The use of the distance \bar{D} in ref. 99 was appropriate because the two parameters R and θ used to parametrize the DS specified the location of phase points in the (Q_1, Q_2) plane

(index 2 case). Conservation of energy together with the minimum distance condition then served to define the corresponding momenta (P_1, P_2) .

If we use the parametrization of the hyperbolas of eq. (A3) and (A4) it is more natural to introduce a new distance defined in the full phase space (cf. eq. (3.12)):

$$D = \frac{1}{4} \sum_{i=1}^k (Q_i^2 + P_i^2). \quad (\text{A6})$$

The derivatives with respect to time of the two distances \bar{D} and D are in fact *identical*, so that for both cases the minimum distance condition is:

$$\dot{D} = \sum_{i=1}^k \Lambda_i Q_i P_i = 0. \quad (\text{A7})$$

Independent of the sign of I_i , the following equation then defines the constant energy EDS ($K(I_1, \dots, I_n) = E$):

$$\sum_{i=1}^k 2\Lambda_i |I_i| \frac{\tan(t_i)}{\cos(t_i)} = 0. \quad (\text{A8})$$

In terms of the variables $X_i \equiv \tan(t_i)/\cos(t_i)$, we have:

$$\sum_{i=1}^k 2\Lambda_i |I_i| X_i = 0. \quad (\text{A9})$$

As noted above, the EDS is composed of 4^k parts for the case of an index k saddle. For each saddle plane, the hyperbola has four branches, two with $I_i > 0$ and two with $I_i < 0$. The four branches are in 1:1 correspondence with the symbolic notation introduced in Section III:

$$I_i > 0 \text{ and } t_i \in \left] \frac{-\pi}{2}; \frac{\pi}{2} \right[\longleftrightarrow (+; -) \quad (\text{A10a})$$

$$I_i > 0 \text{ and } t_i \in \left] \frac{\pi}{2}; \frac{3\pi}{2} \right[\longleftrightarrow (-; +) \quad (\text{A10b})$$

$$I_i < 0 \text{ and } t_i \in \left] \frac{-\pi}{2}; \frac{\pi}{2} \right[\longleftrightarrow (+; +) \quad (\text{A10c})$$

$$I_i < 0 \text{ and } t_i \in \left] \frac{\pi}{2}; \frac{3\pi}{2} \right[\longleftrightarrow (-; -). \quad (\text{A10d})$$

From the equation $X_i = \tan(t_i)/\cos(t_i)$ we obtain:

$$X_i^2 = \left(\frac{\tan(t_i)}{\cos(t_i)} \right)^2 = \frac{1}{\cos^4(t_i)} - \frac{1}{\cos^2(t_i)}. \quad (\text{A11})$$

which yields

$$z_i^2 - z_i - X_i^2 = 0 \tag{A12}$$

in terms of the new variable $z_i = 1/\cos^2(t_i)$. The discriminant $\Delta = 1 + 4X_i^2$ of eq. (A12) is always positive and there are two roots:

$$(z_i)_\pm = \frac{1 \pm \sqrt{\Delta}}{2}. \tag{A13}$$

However, z is also a square ($z = \cos(t_i)^{-2}$) and the $(z_i)_-$ solution is always negative or zero. So, the only possible solution is actually $(z_i)_+$, so we finally have for t_i the expression:

$$t_i = \cos^{-1} \left[\pm \sqrt{\frac{2}{1 + \sqrt{\Delta}}} \right]. \tag{A14}$$

If we set $\alpha = \sqrt{\frac{2}{1 + \sqrt{\Delta}}}$, we see that $0 \leq \alpha \leq 1$ and $-1 \leq -\alpha \leq 0$ and consequently $\cos^{-1}(\alpha) \in [0; \frac{\pi}{2}]$ and $\cos^{-1}(-\alpha) \in [\frac{\pi}{2}; \pi]$. It is straightforward to choose the appropriate root depending on which branch of the hyperbola we are working on and making the appropriate translation of the set $[0; \pi]$ to either $[-\frac{\pi}{2}; \frac{\pi}{2}]$ or $[\frac{\pi}{2}; \frac{3\pi}{2}]$.

To sample the EDS, we first have to fix the value of the energy E , which can be either positive or negative. We must therefore find a set of actions I_i for which eq. (3.11) holds. This can be done by choosing $n - 1$ actions and solving numerically for the value of the last action I_s . This set of actions can be chosen in a systematic way. We can specify maximal or minimal values for each action depending on the part of the EDS we are sampling and sample systematically from zero to the maximal or the minimal value of each actions. The determination of these maximal or minimal values of the actions is related to the accuracy of the normal form Hamiltonian and its associated coordinates transforms (3.2). The check of the accuracy of the normal form Hamiltonian is an important topic and we discuss some aspects of this topic relevant to this work in the next paragraph.

Normal form theory is procedure which enable us to construct a "simple" Hamiltonian which approximates the dynamics of a given Hamiltonian in a neighbourhood of an equilibrium point of this Hamiltonian. The outputs of this procedure are a normal form Hamiltonian and two sets of coordinates transformations which enable us to navigate between the two sets of physical and normal form coordinates. The construction of the normal form Hamiltonian relies on a Taylor expansion about an equilibrium point and a normalisation process which results in the normal form being valid only in a certain neighbourhood of

the equilibrium point under consideration. Therefore we expect the normal form to "break down", i.e. not be an accurate approximation of the physical Hamiltonian, when we leave this neighbourhood. The major question here is how to define this neighbourhood or, in other words, how to measure the accuracy of the normal form? For Hamiltonian systems there is a quite natural measure of the accuracy of the normal form which is the conservation of energy. The idea used here is to compare the energy provided by the normal form Hamiltonian with the energy provided by the initial Hamiltonian and decide a threshold for energy "disagreement" between the two:

$$|E_{ini} - E_{NF}| \leq \epsilon. \quad (\text{A15})$$

For phase space points in normal form coordinates we compute the energy with the normal form Hamiltonian and use the backward transformations (3.2) provided by the normalisation process to obtain phase space points in physical coordinates with which we can compute the energy using the physical Hamiltonian. Starting from phase space points "close" to the equilibrium point, and increasing the distance from this equilibrium point gradually, we can construct a connected set of phase space points for which (A15) holds, and which for the purpose of this work defines the neighbourhood of validity of the normal form. This neighbourhood, denoted \mathcal{L}_ϵ , depends on ϵ . The parameter ϵ actually quantifies the "error threshold" in the normal form. For this work the value of ϵ was taken as a factor 10^{-3} times the physical energy of the energy surface on which the EDS was sampled.

We now return to the problem of computing the maximal or minimal values of the actions. We can differentiate between the case of a saddle mode action and a bath mode action. For a bath mode with action I_b the dynamics is confined to a circle of radius $r = \sqrt{2I_b}$ in this bath mode plane. To determine the maximal value of I_b we set all other coordinates related to the other modes (bath and saddle modes) to zero so that the phase space point is located at the origin of all the mode planes except the one we try to determine the maximum value of the action. For a certain value of the action I_b we calculate the energy ϵ -agreement for samples all around the circle of radius $r = \sqrt{2I_b}$. As we increase the action I_b the radius of the circle will increase and we will find some points on the circle which do not belong to \mathcal{L}_ϵ . So the maximal value of the action I_b will be the one corresponding to the last circle for which all the points on the circle belong to \mathcal{L}_ϵ . For the action corresponding to a saddle mode we can have two cases depending on which part of the EDS we are sampling but the

procedure is quite identical for the two cases. For a saddle mode of fixed action I_s on a certain part of the EDS the dynamics is constrained on one branch of a hyperbola. As for the case of a bath mode we set all coordinates related to the other modes to zero. On the branch of the hyperbola the minimal distance from the origin in the saddle mode plane is at $t = 0$ or π depending on the part of the EDS. So if we fix t to 0 or π and increase ($I_s > 0$) or decrease ($I_s < 0$) we will pass a point for which the energy ϵ -agreement between normal form Hamiltonian energy and initial energy does not hold which means that we have left \mathcal{L}_ϵ . This determines the maximal or minimal value of the action I_s .

Having selected a particular set of bath mode and saddle actions we sample points which belong to the EDS by assigning values to the variables that are complementary to the actions. For each of the bath mode planes we sample the angle variable conjugate to the actions. If a bath mode action is I_b , a conserved quantity, we have $I_b = \frac{1}{2}(q_b^2 + p_b^2)$. The angle θ , $0 \leq \theta \leq 2\pi$, parameterizes a circle of radius $r = \sqrt{2I_b}$ in the (q_b, p_b) plane.

For the saddle planes, we need to solve the minimum distance equation to sample points on the EDS. Equation (A9) provides us with a very simple relation among the variables X_i , $i = 1, \dots, k$. By fixing all of those variables except X_1 and X_2 , for example, equation (A9) describes the equation of a straight line with slope $-\frac{\Lambda_2|I_2|}{\Lambda_1|I_1|}$ and Y -intercept $\sum_{j=3}^k -\frac{\Lambda_j|I_j|}{\Lambda_1|I_1|}X_j$. For the case of only two saddle planes, $k = 2$, it reduces to the equation of a straight line passing through the origin. After determining the X_i , we compute the t_i as explained above and finally the (Q_i, P_i) .

-
- [1] D. Kruger, R. Rousseau, H. Fuchs, and D. Marx, *Angew. Chem. Intl. Ed.* **42**, 2251 (2003).
 - [2] Z. Huang and R. Boulatov, *Pure Appl. Chem.* **82**, 931 (2010).
 - [3] Z. Huang and R. Boulatov, *Chem. Soc. Rev.* **40**, 2359 (2011).
 - [4] S. Konda, J. N. Brantley, C. W. Bielawski, and D. E. Makarov, *J. Chem. Phys.* **135**, 164103 (2011).
 - [5] K. Wiggins, J. Brantley, and C. W. Bielawski, *ACS Macro Lett.* **1**, 623 (2012).
 - [6] O. K. Dudko, *Proc. Nat. Acad. Sci. USA* **106**, 8795 (2009).
 - [7] S. Yohichi and O. K. Dudko, *Phys. Rev. Lett.* **104**, 048101 (2010).
 - [8] O. K. Dudko, T. G. W. Graham, and R. Best, *Phys. Rev. Lett.* **107**, 208301 (2011).

- [9] S. Yohichi and O. K. Dudko, *J. Chem. Phys.* **134**, 065102 (2011).
- [10] D. E. Makarov, *J. Chem. Phys.* **135**, 194112 (2011).
- [11] O. Prezhdo and Y. Pereverzev, *Acc. Chem. Res.* **42**, 693 (2009).
- [12] H.-H. Kausch, *Polymer Fracture* (Springer Verlag, New York, 1987).
- [13] B. Crist, *Ann. Rev. Mater. Sci.* **25**, 295 (1995).
- [14] M. J. Buehler and S. K. S, *Rev. Mod. Phys.* **82**, 1459 (2010).
- [15] Y. Termonia, P. Meakin, and P. Smith, *Macromolecules* **18**, 2246 (1985).
- [16] Y. Termonia and P. Smith, *Polymer* **27**, 1845 (1986).
- [17] L. Garnier, B. Gauthier-Manuel, E. W. van der Vegte, J. Snijders, and G. Hadziioannou, *J. Chem. Phys.* **113**, 2497 (2000).
- [18] A. M. Saitta and M. L. Klein, *J. Phys. Chem. B* **104**, 2197 (2000).
- [19] A. M. Saitta and M. L. Klein, *J. Phys. Chem. A* **105**, 6495 (2001).
- [20] A. M. Maroja, F. A. Oliveira, M. Ciesla, and L. Longa, *Phys. Rev. E* **63**, Art. No. 061801 (2001).
- [21] U. F. Rohrig and I. Frank, *J. Chem. Phys.* **115**, 8670 (2001).
- [22] Y. Suzuki and O. Dudko, *Phys. Rev. Lett.* **104**, 048101 (2010).
- [23] D. Gersappe and M. O. Robbins, *Europhys. Lett.* **48**, 150 (1999).
- [24] A. E. Filippov, J. Klafter, and M. Urbakh, *Phys. Rev. Lett.* **92**, Art. No. 135503 (2004).
- [25] E. Evans, *Ann. Rev. Biophys. Biomol. Struct.* **30**, 105 (2001).
- [26] P. M. Williams, *Anal. Chim. Act.* **479**, 107 (2003).
- [27] S. A. Harris, *Contemp. Phys.* **45**, 11 (2004).
- [28] I. Tinoco, *Ann. Rev. Biophys. Biomol. Struct.* **33**, 363 (2004).
- [29] Y. V. Pereverzev and O. V. Prezhdo, *Phys. Rev. E* **73**, 050902 (2006).
- [30] C. Hyeon and D. Thirumalai, *J. Phys. Condensed Matter* **19**, 113101 (2007).
- [31] S. Kumar and M. S. Li, *Phys. Rept* **486**, 1 (2010).
- [32] E. Fermi, J. Pasta, and S. Ulam, in *Collected papers of Enrico Fermi*, edited by E. Segre (University of Chicago Press, Chicago, 1965), vol. II, pp. 978–989.
- [33] J. Ford, *Phys. Rep.* **213**, 271 (1992).
- [34] H. Schranz, S. Nordholm, and B. Freasier, *Chem. Phys.* **108**, 69 (1986).
- [35] H. Schranz, S. Nordholm, and B. Freasier, *Chem. Phys.* **108**, 93 (1986).
- [36] H. Schranz, S. Nordholm, and B. Freasier, *Chem. Phys.* **108**, 105 (1986).

- [37] M. R. Nyden and D. W. Noid, *J. Phys. Chem.* **95**, 940 (1991).
- [38] B. G. Sumpter and D. W. Noid, *Chem. Phys.* **160**, 393 (1992).
- [39] B. G. Sumpter and D. W. Noid, *Chem. Phys.* **186**, 323 (1994).
- [40] K. Bolton, S. Nordholm, and H. Schranz, *J. Phys. Chem.* **99**, 2477 (1995).
- [41] T. Okabe and H. Yamada, *Mod. Phys. Lett. B* **12**, 901 (1998).
- [42] T. Okabe and H. Yamada, *Mod. Phys. Lett. B* **13**, 303 (1999).
- [43] R. Reigada, A. Sarmiento, A. H. Romero, J. M. Sancho, and K. Lindenberg, *J. Chem. Phys.* **112**, 10615 (2000).
- [44] R. Reigada, A. Sarmiento, and K. Lindenberg, *Phys. Rev. E* **64**, Art. No. 066608 (2001).
- [45] T. Okabe and H. Yamada, *Mod. Phys. Lett. B* **18**, 269 (2004).
- [46] S. Lepri, P. Sandri, and A. Politi, *Eur. Phys. J. B* **47**, 549 (2005).
- [47] P. J. Robinson and K. A. Holbrook, *Unimolecular Reactions* (Wiley, New York, 1972).
- [48] W. Forst, *Theory of Unimolecular Reactions* (Academic, New York, 1973).
- [49] R. G. Gilbert and S. C. Smith, *Theory of Unimolecular and Recombination Reactions* (Blackwell Scientific, Oxford, 1990).
- [50] T. Baer and W. L. Hase, *Unimolecular Reaction Dynamics* (Oxford University Press, New York, 1996).
- [51] W. L. Hase, *Acc. Chem. Res.* **31**, 659 (1998).
- [52] E. P. Wigner, *Trans. Faraday Soc.* **34**, 29 (1938).
- [53] J. C. Keck, *Adv. Chem. Phys.* **XIII**, 85 (1967).
- [54] P. Pechukas, *Ann. Rev. Phys. Chem.* **32**, 159 (1981).
- [55] D. G. Truhlar, W. L. Hase, and J. T. Hynes, *J. Phys. Chem.* **87**, 2664 (1983).
- [56] J. B. Anderson, *Adv. Chem. Phys.* **XCI**, 381 (1995).
- [57] D. G. Truhlar, B. C. Garrett, and S. J. Klippenstein, *J. Phys. Chem.* **100**, 12711 (1996).
- [58] A. I. Mel'ker, A. I. Mikhailin, and N. Y. Zolotarevskii, *Sov. Phys. Solid State* **21**, 890 (1979).
- [59] A. I. Mel'ker and T. Kuznetsova, *Sov. Phys. Solid State* **22**, 606 (1980).
- [60] A. I. Mikhailin and A. I. Mel'ker, *Sov. Phys. Solid State* **22**, 1472 (1980).
- [61] A. I. Mel'ker and A. I. Mikhailin, *Sov. Phys. Solid State* **23**, 1016 (1981).
- [62] R. W. Welland, M. Shin, D. Allen, and J. B. Ketterson, *Phys. Rev. B* **46**, 503 (1992).
- [63] F. A. Oliveira and P. L. Taylor, *J. Chem. Phys.* **101**, 10118 (1994).
- [64] K. L. Sebastian and R. Puthur, *Chem. Phys. Lett.* **304**, 399 (1999).

- [65] R. Puthur and K. L. Sebastian, *Phys. Rev. B* **66**, 024304 (2002).
- [66] A. Sain, C. L. Dias, and M. Grant, *Phys. Rev. E* **74**, Art. No. 046111 (2006).
- [67] A. Ghosh and D. Dimitrov, *J. Chem. Phys.* **132**, 204902 (2010).
- [68] J. Paturej, A. Milchev, V. Rostiashvili, and T. Vilgis, *EPL* **94**, 48003 (2011).
- [69] J. N. Stember and G. S. Ezra, *Chem. Phys.* **337**, 11 (2007).
- [70] J. N. Stember and G. S. Ezra, *Chem. Phys.* **381**, 80 (2011).
- [71] S. Wiggins, *Physica D* **44**, 471 (1990).
- [72] S. Wiggins, L. Wiesenfeld, C. Jaffe, and T. Uzer, *Phys. Rev. Lett.* **86(24)**, 5478 (2001).
- [73] T. Uzer, C. Jaffe, J. Palacian, P. Yanguas, and S. Wiggins, *Nonlinearity* **15**, 957 (2002).
- [74] H. Waalkens, A. Burbanks, and S. Wiggins, *J. Phys. A* **37**, L257 (2004).
- [75] H. Waalkens and S. Wiggins, *J. Phys. A* **37**, L435 (2004).
- [76] H. Waalkens, A. Burbanks, and S. Wiggins, *J. Chem. Phys.* **121**, 6207 (2004).
- [77] H. Waalkens, A. Burbanks, and S. Wiggins, *Physical Review Letters* **95**, 084301 (2005).
- [78] H. Waalkens, A. Burbanks, and S. Wiggins, *J. Phys. A* **38**, L759 (2005).
- [79] R. Schubert, H. Waalkens, and S. Wiggins, *Phys. Rev. Lett.* **96**, 218302 (2006).
- [80] H. Waalkens, R. Schubert, and S. Wiggins, *Nonlinearity* **21**, R1 (2008).
- [81] R. S. MacKay, *Phys. Lett. A* **145**, 425 (1990).
- [82] T. Komatsuzaki and R. S. Berry, *J. Mol. Struct. THEOCHEM* **506**, 55 (2000).
- [83] T. Komatsuzaki and R. S. Berry, *Adv. Chem. Phys.* **123**, 79 (2002).
- [84] L. Wiesenfeld, A. Faure, and T. Johann, *J. Phys. B* **36**, 1319 (2003).
- [85] L. Wiesenfeld, *J. Phys. A* **37**, L143 (2004).
- [86] L. Wiesenfeld, *Few Body Syst.* **34**, 163 (2004).
- [87] T. Komatsuzaki, K. Hoshino, and Y. Matsunaga, *Adv. Chem. Phys.* **130 B**, 257 (2005).
- [88] C. Jaffé, S. Kawai, J. Palacian, P. Yanguas, and T. Uzer, *Adv. Chem. Phys.* **130 A**, 171 (2005).
- [89] L. Wiesenfeld, *Adv. Chem. Phys.* **130 A**, 217 (2005).
- [90] F. Gabern, W. S. Koon, J. E. Marsden, and S. D. Ross, *Physica D* **211**, 391 (2005).
- [91] F. Gabern, W. S. Koon, J. E. Marsden, and S. D. Ross, *Few-Body Systems* **38**, 167 (2006).
- [92] A. Shojiguchi, C. B. Li, T. Komatsuzaki, and M. Toda, *Comm. Nonlinear Sci. Numerical Simulation* **13**, 857 (2008).
- [93] Consider a potential energy function $V = V(q_1, \dots, q_n)$ that is a function of n coordinates

- $\{q_k\}$. (Coordinates describing translation and rotation are excluded.) At a non-degenerate critical point of V , where $\partial V/\partial q_k = 0$, $k = 1, \dots, n$, the Hessian matrix $\partial^2 V/\partial q_i \partial q_j$ has n nonzero eigenvalues. The *index* of the critical point is the number of negative eigenvalues.
- [94] P. G. Mezey, *Potential Energy Hypersurfaces* (Elsevier, Amsterdam, 1987).
- [95] D. J. Wales, *Energy Landscapes* (Cambridge University Press, Cambridge, 2003).
- [96] G. S. Ezra and S. Wiggins, *J. Phys. A* **42**, 205101 (2009).
- [97] G. Haller, J. Palacian, P. Yanguas, T. Uzer, and C. Jaffé, *Comm. Nonlinear Sci. Num. Simul.* **15**, 48 (2010).
- [98] G. Haller, T. Uzer, J. Palacian, P. Yanguas, and C. Jaffé, *Nonlinearity* **24**, 527 (2011).
- [99] P. Collins, G. S. Ezra, and S. Wiggins, *J. Chem. Phys.* **134**, 244105 (2011).
- [100] L. Harding, S. Klippenstein, and A. Jasper, *J. Phys. Chem. A* **116**, 6967 (2012).
- [101] B. Andrews and W. Chesnavich, *Chem. Phys. Lett.* **104**, 24 (1984).
- [102] M. Grice, B. Andrews, and W. Chesnavich, *J. Chem. Phys.* **87**, 959 (1987).
- [103] P. Morse, *Phys. Rev.* **34**, 57 (1929).
- [104] S. Wiggins, *Normally hyperbolic invariant manifolds in dynamical systems* (Springer-Verlag, 1994).
- [105] H. Eyring, *Chem. Rev* **17**, 65 (1935).

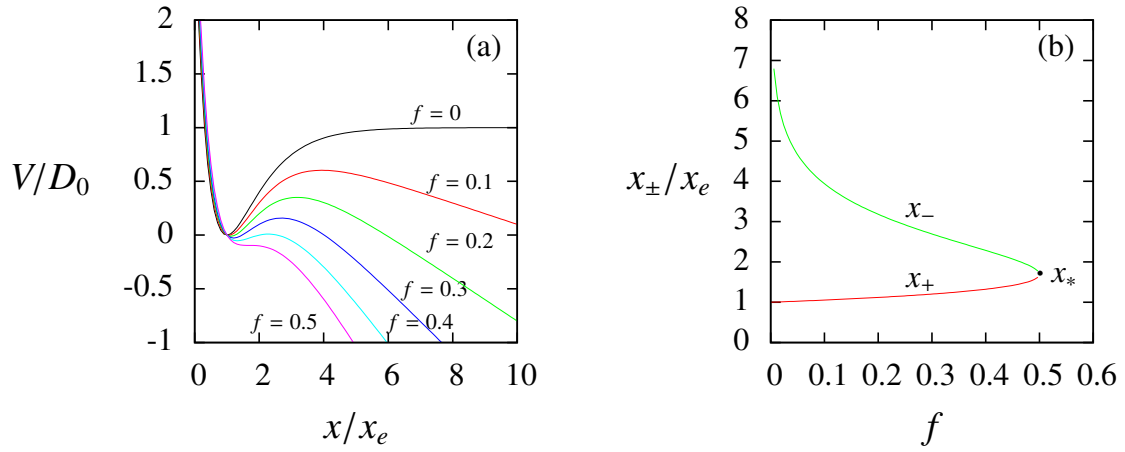


FIG. 1: (a) Potential function of eq. (2.1) for different values of the force parameter f . (b) Locations of the equilibrium points of the 1 dof Hamiltonian (2.1) as a function of the force parameter f .

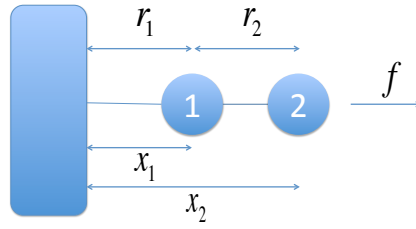


FIG. 2: Definition of ‘external’ (space-fixed) coordinates (x_1, x_2) and ‘internal’ (bond) coordinates (r_1, r_2) for the $n = 2$ atom Morse chain.

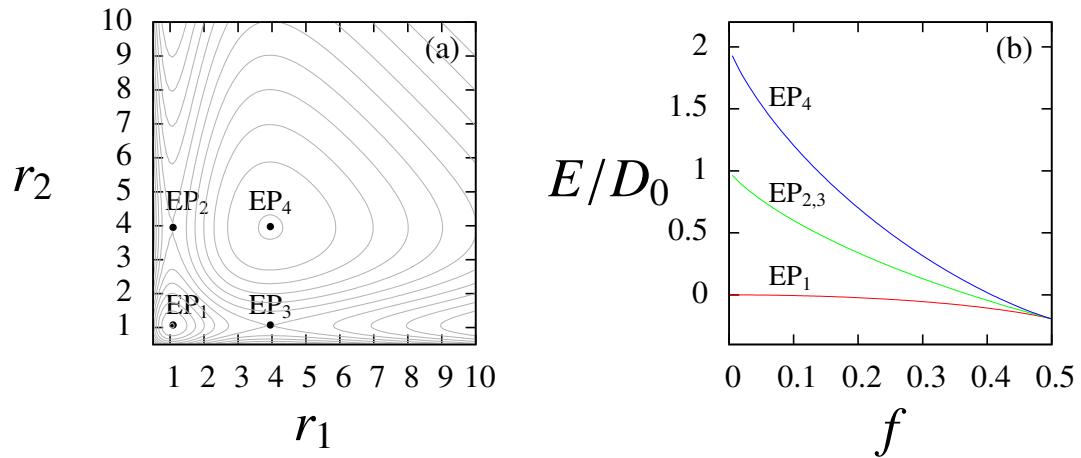


FIG. 3: (a) Contour plot of the potential energy surface for the $n = 2$ Morse chain with $f = 0.1$.
(b) Energies of the different equilibria as a function of the force parameter f .

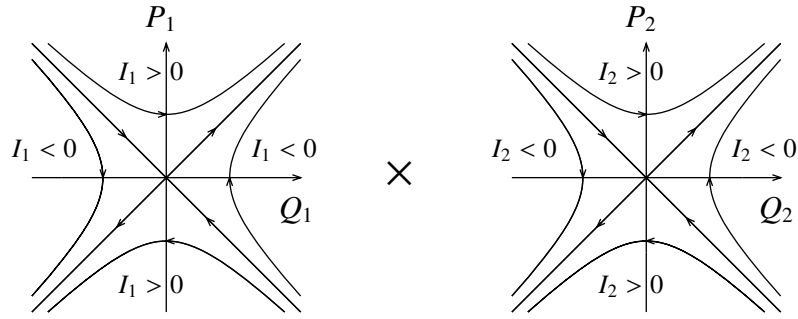


FIG. 4: Schematic representation of the dynamics in the two saddle planes in physical normal form coordinates.

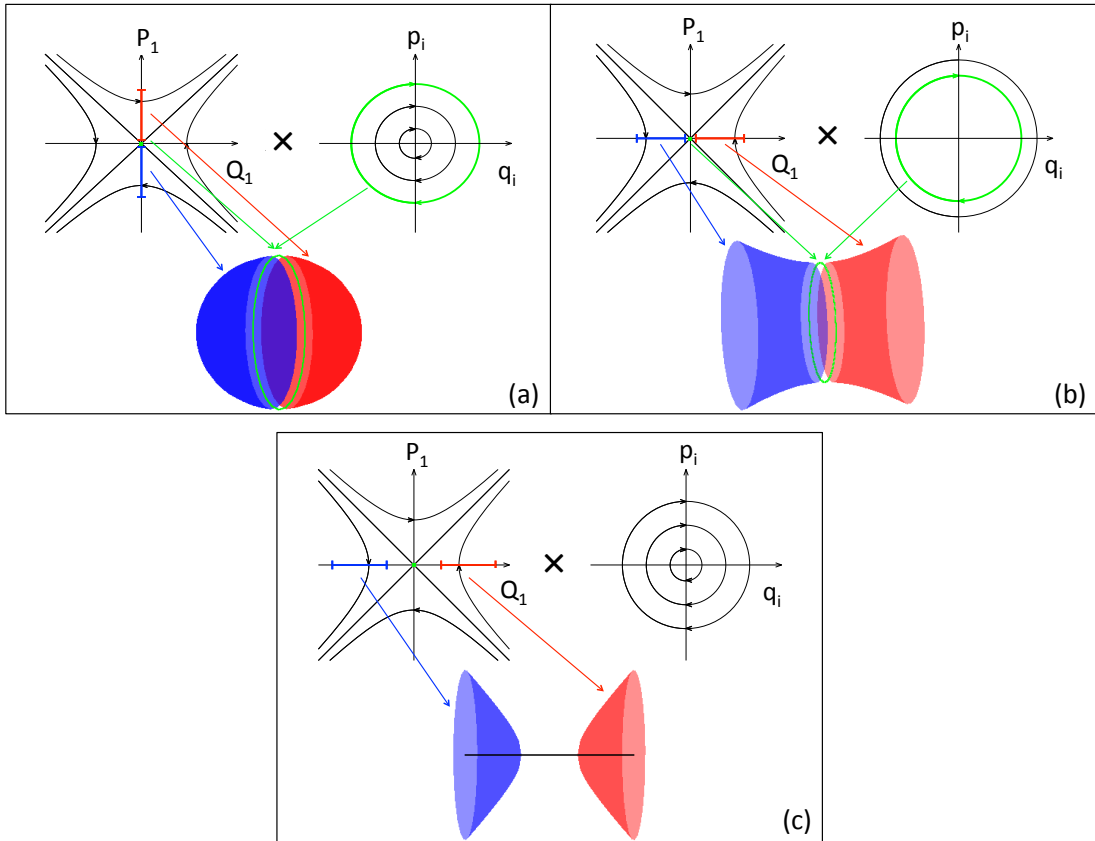


FIG. 5:

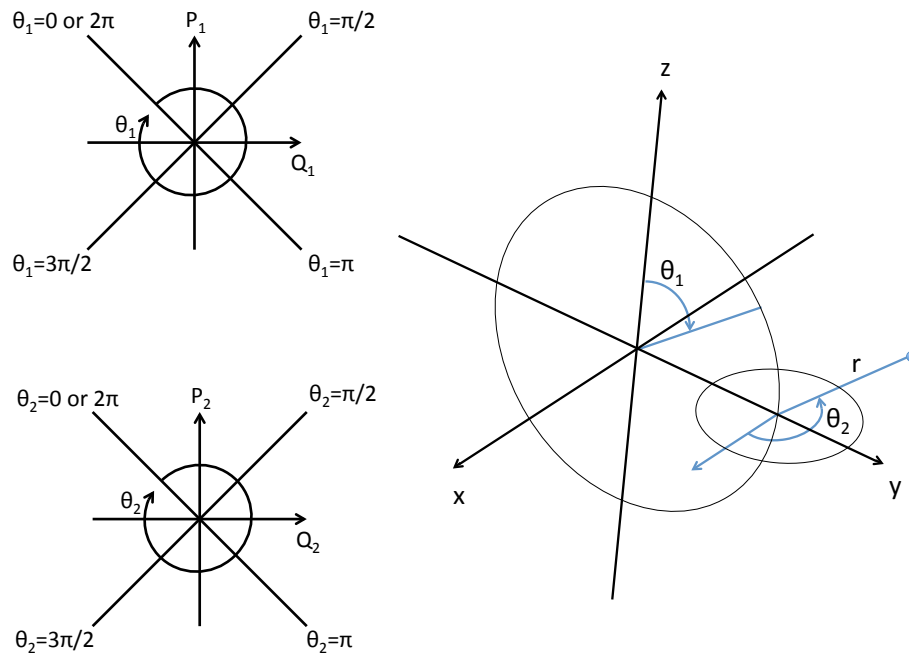


FIG. 6: Toroidal representation of the extended dividing surface.

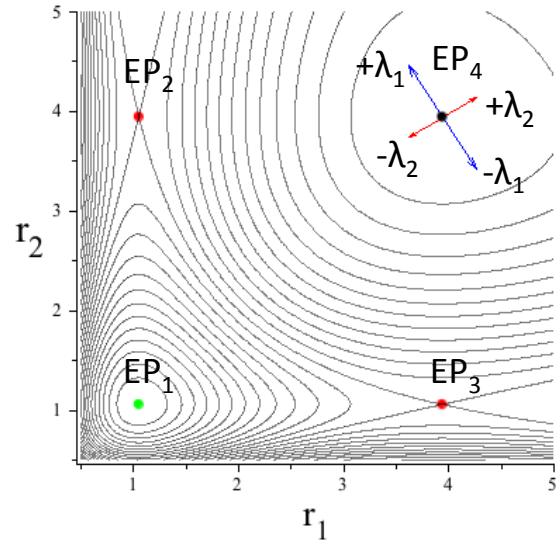


FIG. 7: Potential energy contours and projections of eigenvectors obtained by linearizing Hamilton's equations about the equilibrium point EP_4 .

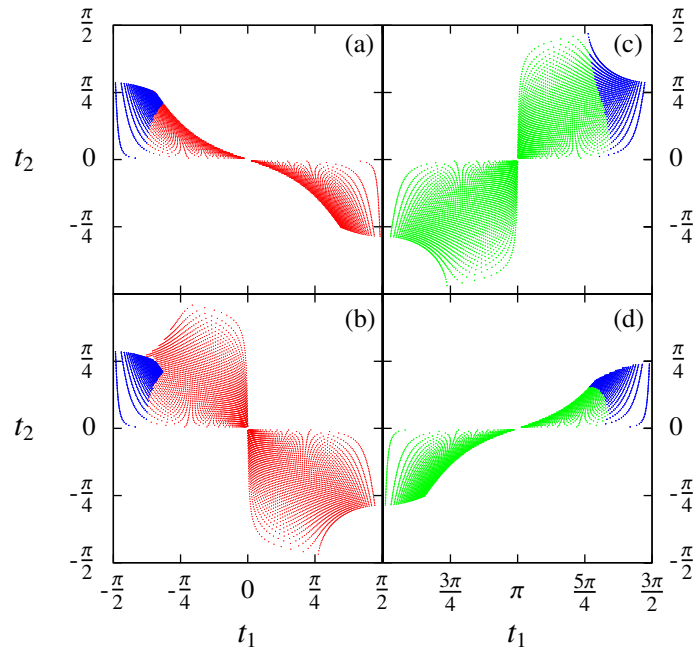


FIG. 8: Subsets of the EDS, labelled by symbol codes $(f_1+; i_1-)$. (a) $(++; +-)$. (b) $(++; --)$. (c) $(-+; +-)$. (d) $(-+; --)$.

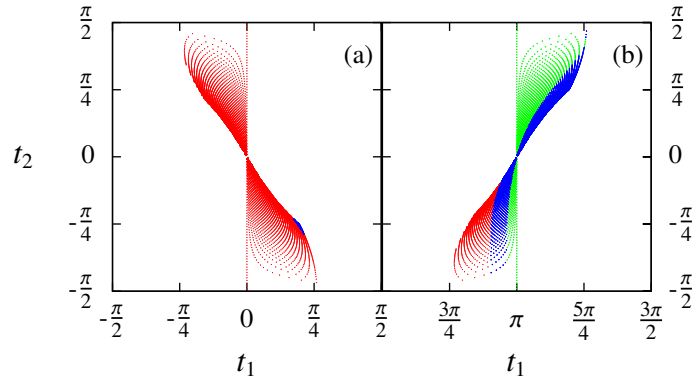


FIG. 9: Subsets of the EDS $(f_{1+}; i_{1+})$. (a) $(++; -+)$. (b) $(-+; ++)$.

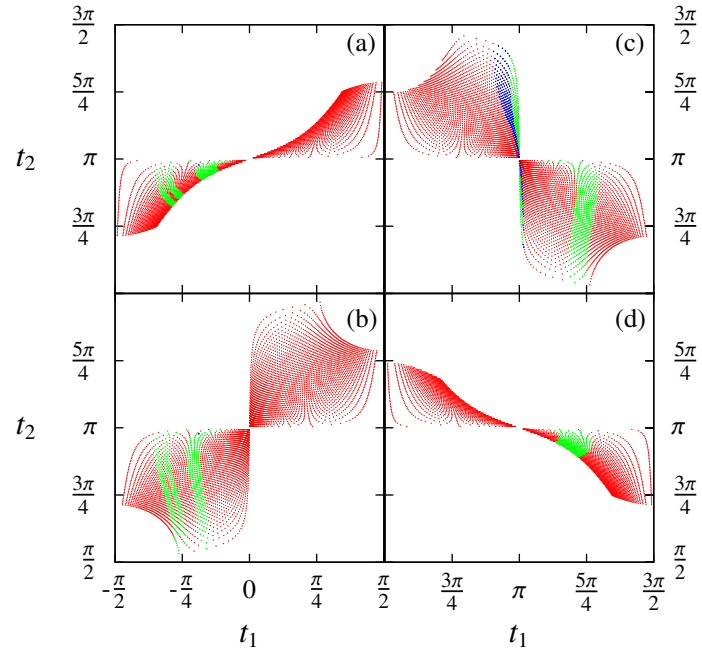


FIG. 10: Subsets of EDS $(f_1-; i_1+)$. (a) $(+-; ++)$. (b) $(+-; --)$. (c) $(--; ++)$. (d) $(--; -+)$.

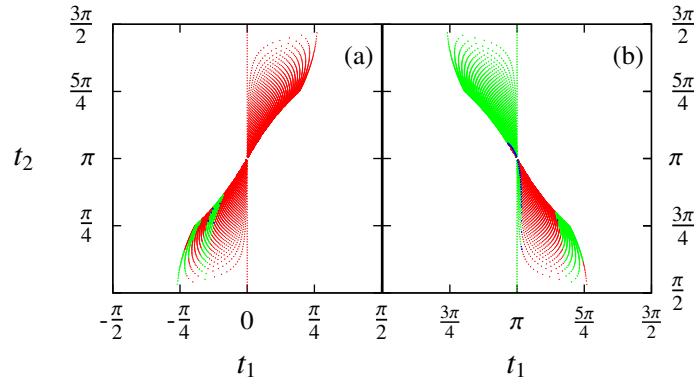


FIG. 11: Subsets of EDS $(f_1-; i_1-)$. (a) $(+-; --)$. (b) $(--; +-)$.

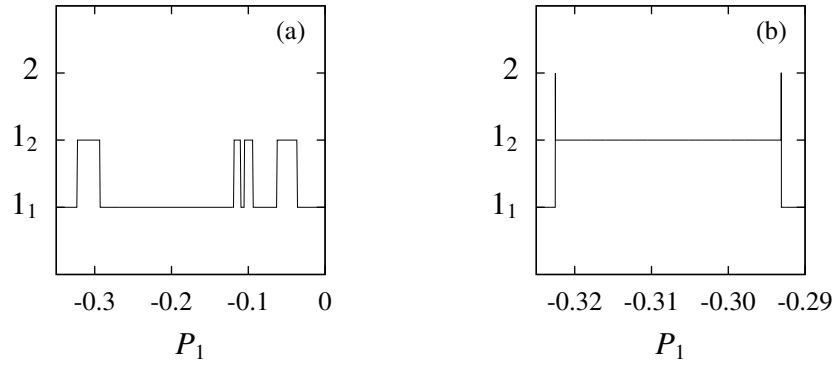


FIG. 12: (a) Trajectory type as a function of location along the 1D cut of the EDS: $Q_1 = 0.2$, $P_1 = -0.35-0.0$, $E = 0.03$. (b) Magnified segment showing the appearance of type 2 trajectories at the boundary between type 1₁ and 1₂.

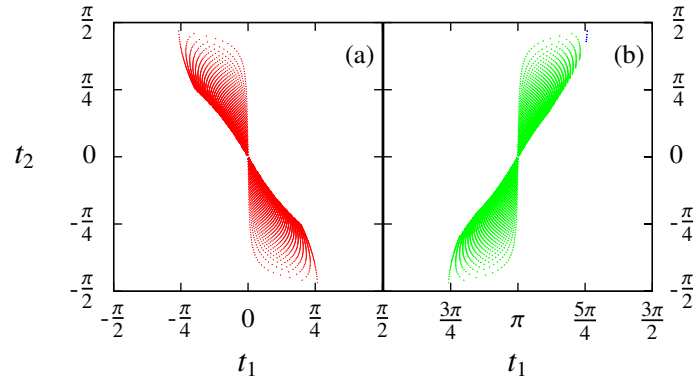


FIG. 13: EDS subsets $(f_1+; i_1-)$. (a) $(++; +-)$. (b) $(-+; --)$.

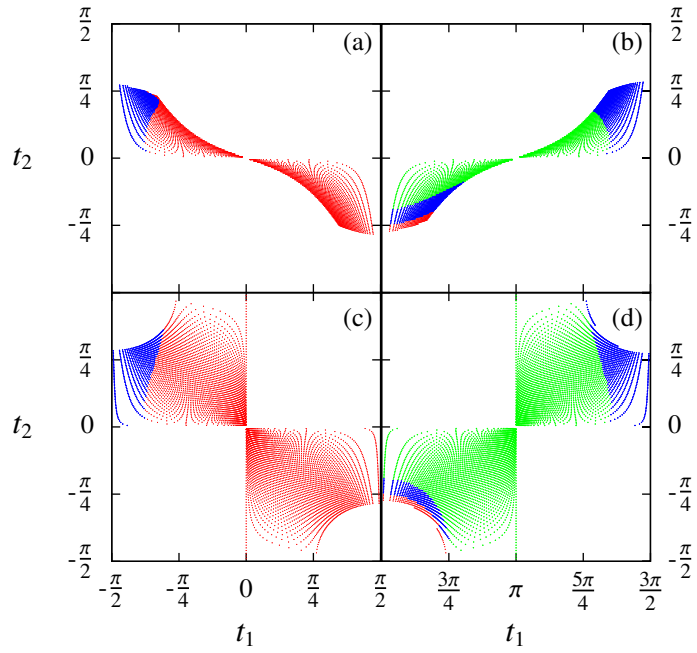


FIG. 14: EDS subsets $(f_1+; i_1+)$. (a) $(++; -+)$. (b) $(-+; ++)$. (c) $(++; ++)$. (d) $(-+; -+)$.

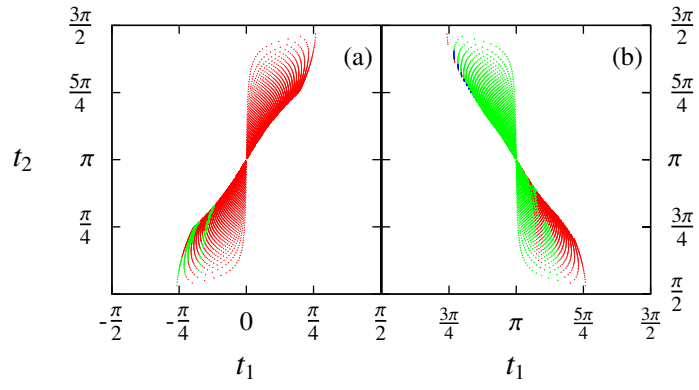


FIG. 15: EDS subsets $(f_1-; i_1+)$. (a) $(+-; ++)$. (b) $(--; -+)$.

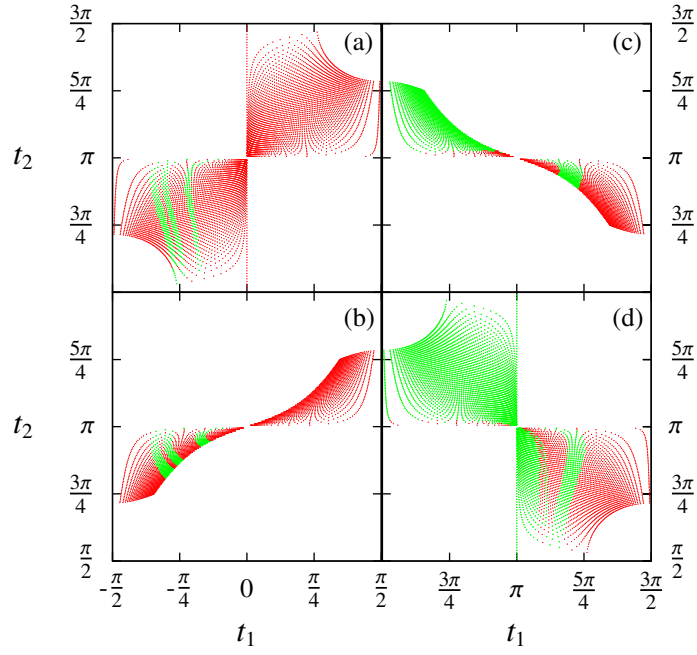


FIG. 16: EDS subsets $(f_1-; i_1-)$. (a) $(+-; +-)$. (b) $(+-; --)$. (c) $(--; +-)$. (d) $(--; --)$.

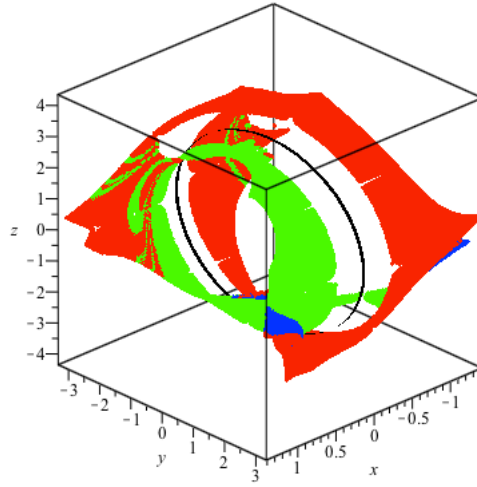


FIG. 17: Global representation of the EDS using the toroidal representation. Energy $E = -0.03$.

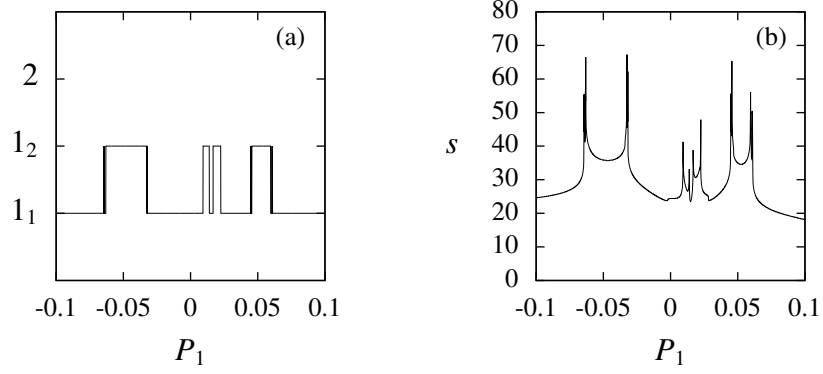


FIG. 18: (a) Trajectory type as a function of location along the 1D cut of the EDS: $Q_1 = 0, P_1 = -0.1-0.1, E = -0.03$. (b) Trajectory exit time s in time units along the cut.

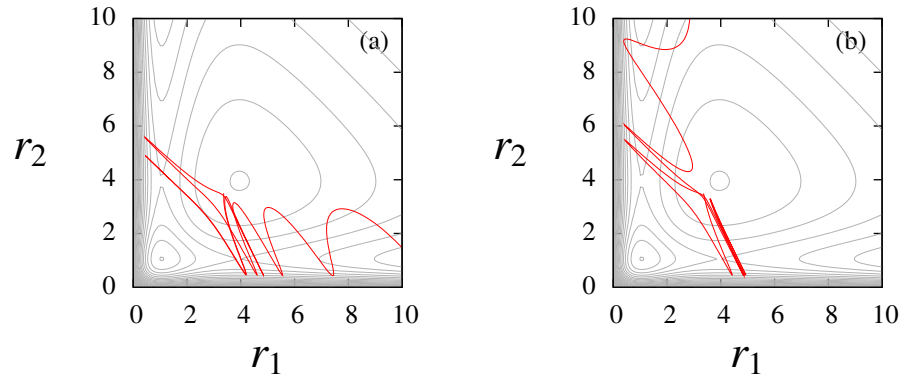


FIG. 19: Examples of trajectories exhibiting the phenomenon of ‘bond healing’.